Variation in predicting pantograph-catenary interaction contact forces, numerical simulations and field measurements

Petter Nåvik[a], Anders Rønnquist[a] and Sebastian Stichel[b]
[a] Norwegian University of Science and Technology, Department of Structural Engineering, Trondheim, Norway
[b]KTH Royal Institute of Technology, Department of Aeronautical and Vehicle Engineering, Stockholm, Sweden

Corresponding author: Petter Nåvik, Department of Structural Engineering, Norwegian University of Science and Technology, Rich. Birkelandsvei 1A, 7491 Trondheim, Norway, petter.r.navik@ntnu.no, +47 73 59 47 00

Anders Rønnquist, Department of Structural Engineering, Norwegian University of Science and Technology, Rich. Birkelandsvei 1A, 7491 Trondheim, Norway, anders.ronnquist@ntnu.no, +47 73 59 47 00

Sebastian Stichel, Department of Aeronautical and Vehicle Engineering, Royal Institute of Technology, SE-100 44 Stockholm, Sweden, stichel@kth.se, +46-70-233 01 63

Abstract

The contact force between the pantograph and the contact wire ensures energy transfer between the two. Too small of a force leads to arching and unstable energy transfer, while too large of a force leads to unnecessary wear on both parts. Thus, obtaining the correct contact force is important for both field measurements and estimates using numerical analysis. The field contact force time series is derived from measurements performed by a self-propelled diagnostic vehicle containing overhead line recording equipment. The measurements are not sampled at the actual contact surface of the interaction but by force transducers beneath the collector strips. Methods exist for obtaining more realistic measurements by adding inertia and aerodynamic effects to the measurements. The variation in predicting the pantograph-catenary interaction contact force is studied in this paper by evaluating the effect of the force sampling location and the effects of signal processing such as filtering. A numerical model validated by field measurements is used to study these effects. First, this paper shows that the numerical model can reproduce a train passage with high accuracy. Second, this study introduces three different options for contact force predictions from numerical simulations. Third, this paper demonstrates that the standard deviation and the maximum and minimum values of the contact force are sensitive to a low-pass filter. For a specific case, an 80 Hz cut-off frequency is compared to a 20 Hz cut-off frequency, as required by EN 50317:2012; the results show an 11% increase in standard deviation, a 36% increase in the maximum value and a 19% decrease in the minimum value.

Keywords: The pantograph-catenary interaction, contact force, field measurements, finite element model, railway catenary system, numerical simulations.

1 Introduction

One of the most important requirements of electric railway operations is a precise and reliable interaction between the railway catenary systems and the pantograph. This contact ensures that the train receives power and is essential for a reliable supply of electrical energy (1). The complexity of this interaction increases with increasing speed (2). The magnitude of the force is important for displacements in the cable system, wear, and maintaining electric power supply. Numerous studies have used the contact force as one of the main evaluation parameters (3–7). Control strategies are based on contact forces (8,9), and the assessment of numerical models is based on contact force measurements (10–12). The mechanical friction resulting from the magnitude of the contact force is one of the three main contributors to wear (13). Therefore, it is important to study not only the magnitude of the force but also the methods used to predict this magnitude and the effects of post-processing.

Numerical models of structures can perform tests and analyses that are not reasonable or even possible to perform on a real structure, either because too many tests are needed or because it is too expensive or simply not feasible. The latter is true for the contact pressure between the contact wire and the pan head. To achieve reliable results, a numerical model must represent the physical processes as accurately as possible. In particular, the variation of the contact force requires a detailed description of both the pantograph and the catenary. The higher the train speed used in the analysis is, the higher the sample frequency should be. Note that a simple clamp for a dropper can be as small as 2.5 cm long, and to be sure that the collector strips in the model hits it at a speed of only 130 km/h one need a time increment of 0.00069 s, i.e., a frequency of 1444 Hz, and for a speed of 300 km/h, a time increment of 0.0003 s (i.e., 3333 Hz) is needed. However, important results can be obtained with a lower sampling frequency,

but it demonstrates that a very short time increment is required to study the contact force in detail. In contrast, the measurements with an overhead line recording train from the continuous load process contain response contributions that are also excited at much higher frequencies than the sampling frequency. Currently, the EN 50317:2012 (14) code requires a sampling rate of greater than 200 Hz for a time sampling and of less than 0.4 m for distance sampling for on-line measurements; in addition, the contact forces should be low-pass filtered at 20 Hz, which has been followed by the literature (15) . However, Collina and Bruni (16) state that numerical models should be validated up to at least 100 Hz to describe wear phenomena.

This study focuses on the variation in the predicted contact force of the pantograph-catenary interaction. Both field measurements and numerical results are included in this study. The contact force field measurements are obtained from a database containing measurements taken twice a year for the past five years; these data are sampled every 0.5 m using an overhead line recording vehicle, and the values are taken from force transducers located just beneath the collector strips. This paper presents a finite element numerical model with geometry based on in-field mounting procedures. The model presented here is based on an earlier version of the model discussed in (17,18): it is a three-dimensional model where the train can be given displacements in all three directions and rotational movements about the longitudinal axis of the train and the axis perpendicular to the track. Thus, the track cant can be described along with the horizontal movement of the train. The model includes a description of the contact at the interface between the contact wire and the pan head and considers how the pantographs tilt with the train on curves. The penalty method is used to represent the sliding contact and is the most frequently used method in the literature (19). In this study, the numerical model is validated against geometry, elasticity, pre-sag, displacement time series, frequency content and statistical contact force values from field measurements. The validation shows that the model has sufficient accuracy; the methods used for validation and the sampling procedures for the field measurements are developed in (20–22).

This study focuses on variations in the predicted pantograph-catenary interaction contact force. First, the variation of the measured contact force time series is investigated by studying several passages at the same railway catenary section. The variation is found to be significant, demonstrating the importance of evaluating more than one train passage when conducting field measurements. Second, the effect of post-processing on the contact force prediction is studied using numerical simulations. The differences between three different methods for predicting the contact force are investigated by comparing their mean values, standard deviations, and maximum and minimum values. In addition, the effect of filtering is studied in more detail by comparing the statistical values obtained from a single contact force time series that has been low-pass filtered at varying cut-off frequencies. This study demonstrates that the method used for the low-pass filtering and the limit for the cut-off filter significantly affect the contact force estimations. Overall, this study shows significant variability in the contact force depending on individual train passages and post-processing.

2 Finite element modelling

2.1 Catenary

The finite element method (FEM) is used to numerically model railway catenary sections. This study uses the commercial FEM software Abaqus to create the models and run the simulations.

The first step in the modelling procedure is to obtain the correct geometry of a railway catenary section. Here, this process follows the actual mounting procedure used when installing these sections on site. First, the geometry of the section is defined using only the lengths of the components described in the design. The droppers are created with small geometrical imperfections, a sine wave shape with a very small amplitude, to ensure lateral bending if exposed to pressure. Including dropper slackening is considered to substantially influence the accuracy of the model (19). The second step is to apply the tension forces used on the particular section and to apply gravity; it is important to apply the tension forces and gravity simultaneously to ensure a stable solution that includes geometrical nonlinearities in the process. The resulting geometry should be the same as the on-site geometry. Thus, this procedure ensures accurate geometry without needing further corrections. This procedure is critical when working with three-dimensional section models that have complex geometry and geometrical nonlinearities, considering different span lengths, curves and variable contact wire height. The tension forces in the wires are introduced using predefined temperature loads; it is very important that these tension forces are correct in the model to ensure accurate results (17). The tension force in the stitch wires has been found to be essential for correctly describing the geometry; small variations in the tension force results in large variations in the vertical geometry and thus in the pre-sag and elasticity. This variation is particularly noticeable when modelling the geometrically varying sections, and iterations are therefore needed for each stitch wire to obtain the correct tension force. The iteration procedure is independent of the model and is only dependent on the designed tension force. It is also important to define local coordinate systems at each pole support to ensure correct boundary conditions; this is especially important in sections with curves where an incorrect description leads to erroneous boundary

conditions, which in turn decreases the tension force in the contact and messenger wire due to fixing the wires partly in the wrong direction. This issue does not occur on straight sections because the local coordinate system (CSYS) on the poles is the same as the global CSYS.

The contact wire, messenger wire, stitch wires and droppers are made using three-dimensional deformable beam elements. All wire components are modelled using Timoshenko beam elements, which is preferable for the numerical stability in this particular model, as described in (18), and the shortest wire element length used is 0.05 m. Every light steady arm is modelled with a spring and a point mass, and a point mass is included for every dropper clamp. Finally, a good damping description is very important, as shown in the recent numerical benchmark presented in (19). The Rayleigh damping coefficients estimated from the field measurements in Nåvik et al. (23) are used in this study. The mass and stiffness proportional damping coefficients are α=0.062 and β=6.13e-06, respectively.

The railway catenary section in the present study is located along the Dovre rail line and is named "Fokstua wire 21". This is a 1295 m long section of railway with a catenary system called System 20 C1 (24). The key properties of this section are presented in **Table 1** and **Table 2**.

Table 1. Key properties of the catenary section Fokstua wire 21

Section	Fokstua
Length	1295 m
Year of construction	2015
Catenary system	System 20 C1
Tension force in the contact wire	13 kN
Tension force in the messenger wire	13 kN
Cross-sectional area of the contact wire	120 mm^2
Cross-sectional area of the messenger wire	70 mm^2
Density of the wire material	8890 kg/m^3
Wave propagation speed	397 km/h
Stitch wire (Yes/No)	Yes
Number of spans in contact with the pantograph	28

Table 2. Design properties of the Fokstua wire 21 span lengths and droppers

Span no.	**1**	**2**	**3**	**4**	**5**	**6**	**7**	**8**	**9**	**10**	**11**	**12**	**13**	**14**
Length [m]	44.27	44.98	45	49.45	45.51	45.65	44.88	45.03	45.1	44.54	45.28	44.76	45.34	48.87
No. of droppers	2	4	5	5	5	5	5	5	5	5	5	5	5	5
Span no.	**15**	**16**	**17**	**18**	**19**	**20**	**21**	**22**	**23**	**24**	**25**	**26**	**27**	**28**
Length [m]	49.02	48.77	50.8	52.23	51.95	52.1	51.87	52	52.06	42.48	39.95	30.99	39.54	42.55
No. of droppers	5	5	5	6	5	6	5	5	6	5	4	4	4	2

2.2 Pantograph

The numerical model of the pantograph used in this study is a modified version of one with two degrees of freedom (DOF), resulting in five DOFs. The original mass-spring-damper system is obtained from the manufacturer, Schunk Nordiska AB, as presented in **Figure 1** a). This model does not account for the fact that there are two collector strips with two attachment points each, four points in total, or the effect of the stagger. The model is therefore modified to account for these properties. The model includes two collector strips connected to the middle mass with two spring-dampers each. In addition, the original total pan head mass in divided into four, one in each attachment point to account for inertia. The collector strips are modelled as rigid beam elements. The new model is presented in **Figure 1** b) and **Table 3**. The new model meets the requirements of EN 50318 (25).

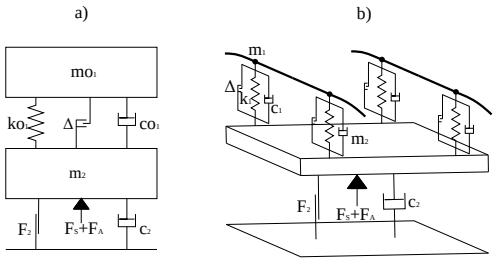

Figure 1. Schematics of the pantograph numerical models: a) the original model and b) the new model

Table 3. Parameters for the pantograph numerical models

Pantograph	**WBL85**	**WBL88**
mo_1 [kg]	4.6	6.6
m_1 [kg]	1.15	1.65
m_2 [kg]	16.5	19.7
ko_1 [N/m]	6200	4400
k_1 [N/m]	1550	1100
Δ [m]	0.035	0.03
co_1 [Ns/m]	20	75.6
c_1 [Ns/m]	5	18.9
c_2 [Ns/m]	63.5	63.5
F_2 [N]	7	17
F_S [N]	55	55
F_A [N]	$0.0068*v(m/s)^2$	$0.0068*v(m/s)^2$

The movement of the train, or, more accurately, the movement of the pantograph, along the investigated sections must be described correctly. The pantograph tilts with the train in curves; due to the horizontal geometry of the contact wire, either stagger or curvature of the track results in the contact wire moving from side to side over the pan head. Two different CSYSs have been used to describe the true movement of the train as it runs along the rail line: one global CSYS (GCSYS) and one local CSYS (LCSYS) in the pantograph. The GCSYS is used to describe the position and rotation of the base of the train. Translational and rotational movements can be prescribed in and about three axes to ensure that the train can follow any track geometry. The train position also rotates to ensure that the pan head is perpendicular to the track at all times. Rotational movements about the longitudinal axis, accounting for the track cant, are introduced by applying the real cant angle described in the design of the rail track geometry. The LCSYS is mainly introduced to ensure that the pantograph moves correctly locally which means that it only experiences displacements along its normal axis and that the pan head can rotate about the longitudinal axis of the pantograph, as presented in the left of **Figure 2**, where arrows are used to illustrate the DOFs available in the local CSYS. An overview of both the GCSYS and the LCSYS is illustrated in the right of **Figure 2**.

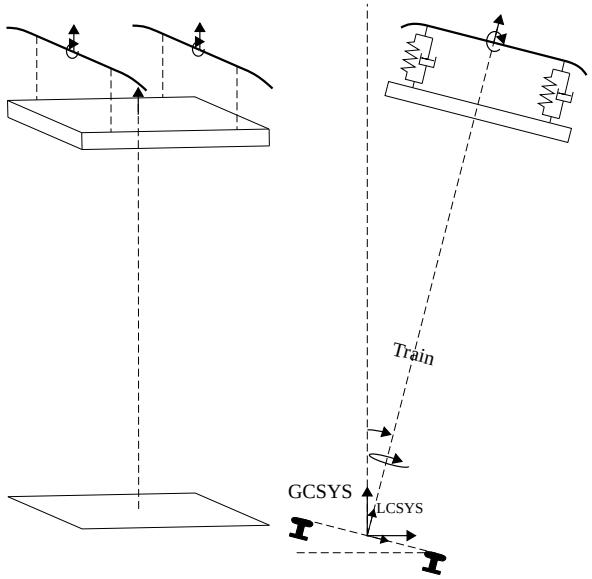

Figure 2. Illustration of the DOFs in the new pantograph model

2.3 Contact

One of the key properties in the catenary evaluation is the description of the contact between the pan head and the contact wire, which results in the important pantograph-catenary interaction. The contact force is dependent on several properties such as the catenary type and design, the pantograph type, the position of the contact wire on the pan heads, the horizontal geometry, and the train speed. Aerodynamic effects on the pantograph related to the train speed are included by adding a correction given by the pantograph manufacturer, as shown in **Table 3**. The importance of adding this is thoroughly shown in (26). Aerodynamic effects related to wind-induced vibration are not included, but their importance is acknowledged in (27).

This model uses a beam-to-beam general contact with hard contact that allows for separation after contact, and the penalty method is used as the constraint enforcement method, which is the default method for this type of contact in Abaqus (28). Ambrósio et al. (29) conclude that the penalty method is suitable for describing all relevant features of the pantograph-catenary interaction contact interface. Frictionless tangential behaviour is assumed.

2.4 Simulation of train passages

Simulating a train travelling along the numerical model is performed as a general nonlinear dynamic analysis and uses implicit time integration to calculate the dynamic response. The Hilbert-Hughes-Taylor α-method is implemented in Abaqus for numerical integration, while Newton's method is used as the numerical technique for solving the nonlinear equilibrium equations. The default value for α is -0.05 to ensure stable solutions with minimum influence on the dynamic system (28). The model uses an automatic incrementation with a maximum time increment size of 0.005 s and a sampling frequency of 200 Hz has been used for this study. An implicit scheme usually gives acceptable solutions with a time step that is typically one or two orders of magnitude larger than the time that an elastic wave uses to cross the smallest element in the model; in contrast, an explicit scheme is only conditionally stable with a step time limit equal to this time (28). At a wave propagation speed equal to the investigated section, which is 435 km/h, and an element length of 0.05 m, a time increment of 0.00041 s is needed to ensure a stable solution when using an explicit scheme.

2.5 Uncertainties/errors in geometric modelling

In the present study, the design values are used to create the numerical models, but it is important to acknowledge that these systems may have changed after they were mounted. This is shown by including both measured and designed contact wire heights from "Fokstua wire 21", as presented in **Figure 3**. This figure illustrates the possible differences between the design and actual geometry, and it clearly shows the variability in the existing structures. Due to these differences, it is easier to validate the geometry by validating the elasticity and pre-sag.

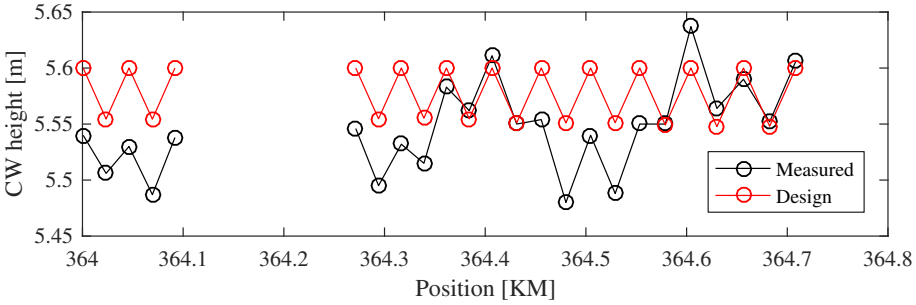

Figure 3. Measured and designed contact wire (CW) heights from Fokstua wire 21

The variability of each train passage, including variability in speed and static uplift force, is neither intended nor currently possible to include in the model. These variations are expected to cause deviations between the results from the model compared to the measured values.

3 Field measurements

In the present investigation, field measurements are used to ensure that the numerical model correctly represents the intended system rendering reliable results. Thus, several different field measurements are performed for comparison between reality and the models. The methods for obtaining these measurements are described in the following section.

3.1 Accelerations

The Fokstua wire 21 was monitored with 10 three-axis wireless accelerometers at selected positions, as shown in **Figure 4**. All sampling is performed at 200 Hz, and the time series are 8 minutes long. The monitoring system used is presented in detail in Nåvik et al. (20). All measurements are sampled during normal scheduled train operation.

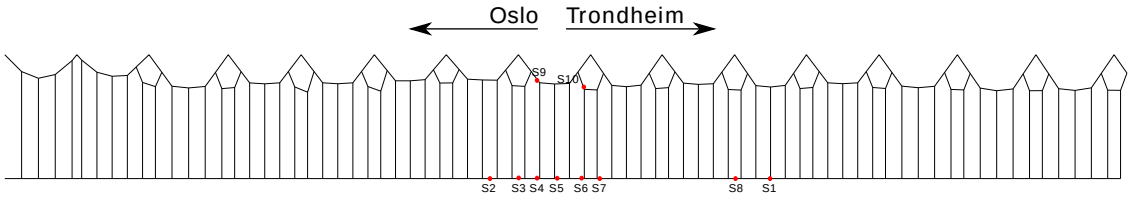

Figure 4. Instrumentation of the Fokstua wire 21, where the red dots illustrate the sensor positions

3.2 Displacements

The estimated displacement time series used in this study is from close-range photogrammetry and from integrated acceleration time series; both methods are thoroughly described in (21). The camera setup for the photogrammetry is aimed at a target on sensor S1. The location of the sensor is in the middle of the span, as shown in **Figure 4**, and the distance between the camera setup and the target is approximately 6 metres. The details of the acceleration measurements are provided in section 3.1.

3.3 Contact forces

All of the contact force field measurements are from scheduled routine measurements with the track and overhead line recording vehicle of the National Norwegian Rail Administration, Mermec Roger 1000 (30). The pantograph on the vehicle is a Schunk WBL85, and all sampling is performed every 0.5 metres along the tracks. The contact forces are measured directly from the force transducers; therefore, the inertia correction described in EN 50317:2012 is not included in the measurements.

3.4 Geometry

The contact wire height and stagger are measured at selected positions along the sections and at positions along the track. The geometry is measured using a laser and a mount, as shown in **Figure 5**. The mount contains three parts: one beam that rests on the rails, one pole that is fastened normal to the beam and can slide along the length of the beam, and a mount on top of the pole for the laser. This setup ensures that the laser is normal to the rail,

and thus, measuring the correct contact wire height directly. In addition, the stagger is read using a ruler on the beam.

Figure 5. Measuring contact wire heights on site

4 Results and discussion

4.1 Parameters of the dynamic simulations

All simulations are performed in the Fokstua wire 21 numerical model for a train running with a single pantograph. To calculate the total uplift force, the static force is set to 55 N, and the aerodynamic force is set according to the formula in the below equation:

$$F\big(v(m/s)\big) = 55 + 0.0068 \times v^2 \text{ N}$$

Simulations are performed with two types of pantographs, WBL85 and WBL88, and with train speeds of 80 and 130 km/h, which give F = 58.36 N and 63.87 N, respectively. Thus, four simulations are performed to represent the train speed on site that more or less falls between these two speeds and these two pantographs are the most commonly used at the investigated section.

4.2 Validation of the numerical model

4.2.1 Geometry and elasticity

It is important to validate the geometry of the numerical models as well as the results they produce. This is challenging because, as mentioned, the geometry varies from span to span and from section to section and often differs considerably from the design, especially for older sections. Instead of comparing exact geometrical values, it is better to look at values such as pre-sag and elasticity. Pre-sag is easy to measure and compare, while elasticity is more time consuming to measure; however, calculated elasticity curves exist for most systems at some specified span length. The elasticity analyses are performed along the length of the numerical models by running a train along the section as a static rather than a dynamic step. The elasticity of the catenary was calculated every 0.11m. The elasticity curve is shown in **Figure 6**; the end spans are not displayed for clarity.

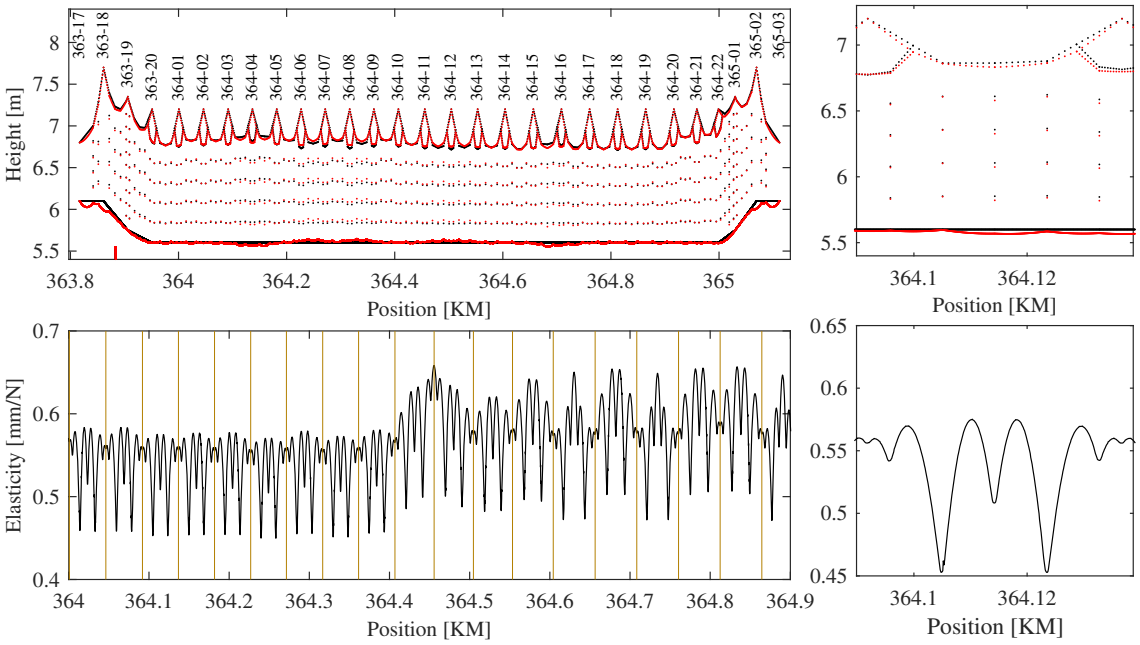

Figure 6. Vertical geometry and elasticity of the numerical model of the railway catenary section Fokstua wire 21. The elasticity of one 44.9 m long span is shown on the right for a clearer interpretation

The elasticity curve to the right in **Figure 6** is compared to an estimated elasticity curve for a 45 m long System 20 C1 span from Banverket's report (31). The elasticity from both of these analyses are approximately equal; the main difference is a slightly stiffer support for the developed numerical model. This difference could be due to the differences in the neighbouring span geometry and other properties.

4.2.2 Dynamic comparison using acceleration and displacement results

A comparison of the measured and simulated displacement time series is performed to verify that the numerical model can produce a satisfactory time series. A displacement time series from the numerical simulation is compared with the displacement measurements from a train passage for further analysis. The numerical results are from an analysis using pantograph WBL88 running at 130 km/h, while the field results are from a typical passenger train passage that normally runs at the same speed of 130 km/h using WBL88. The field displacements are obtained as described in section 3.2. **Figure 7** shows that the displacement time series obtained from the numerical model describes the real response well, including both the displacement magnitude during the whole passage and the shape. The highest peak in the figure is when the train pass the sampling position.

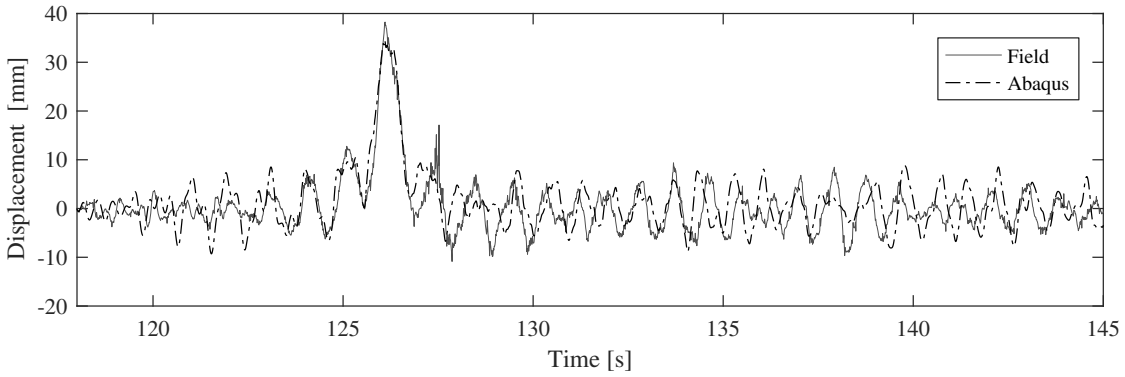

Figure 7. Displacement time series from position S1 with WBL88 at 130 km/h from a numerical simulation and a field displacement estimation for a passing passenger train. The train pass this position at approximately 127 s, as can be seen as a peak in the displacement time series

The frequency content in the dynamic process is also an important quantity that needs to be verified by comparing the results from the numerical simulation with pantograph WBL88 running at 130 km/h with the overall system data from all measurements performed at the location, as described in (20,22). The numerical results are obtained

by calculating the power spectral density (PSD) of the acceleration time series sampled at the corresponding locations to where the sensors were mounted during the field tests.

The mean PSD of the total setup is estimated by normalizing the sum of all sensor contributions by the number of sensors. Thus, a PSD is obtained that can be used to compare the energy magnitude of the process. The field results are obtained by the following procedure: 1) adding the PSDs from all time passages individually for each sensor and normalizing by the number of train passages, giving a mean PSD for each sensor and 2) adding these PSDs from each sensor together and dividing by the number of sensors to obtain a mean total PSD for the section. The result from each location then contributes equally to the section PSD. The frequency content is not expected to be identical due to the randomness in the natural process and because the results from the measured values are averages of many passages; each train passage may differ in terms of speed, pantograph type, wear of the collector strips, wind at the location at each point in time, and temperature. Therefore, the validation is performed through the similarities and the overall behaviour of the dynamic process. Many similar frequencies are expected in the field and numerical analyses, but with varying energy levels, as illustrated by the overall analysis in **Figure 8**, which clearly shows many similar frequencies with some deviating intensities. Furthermore, as expected, some frequency peaks are slightly shifted. Overall, though, taking the nature of the process into account, the comparison is satisfactory.

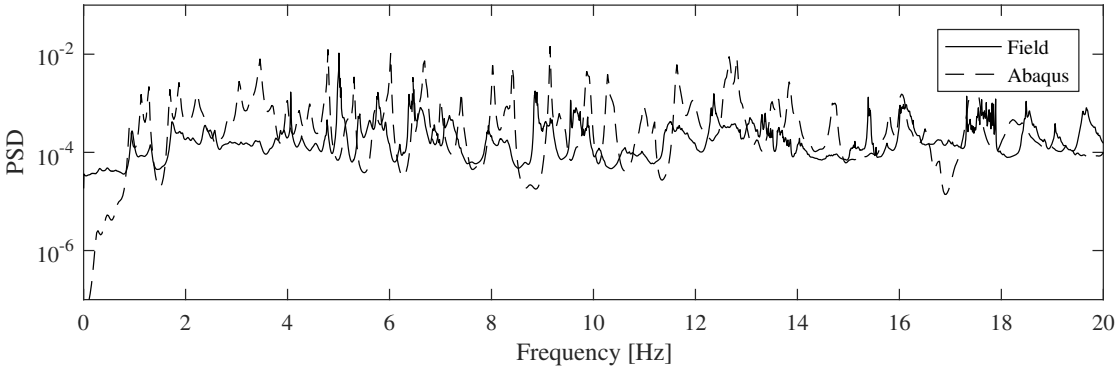

Figure 8. Comparison of the mean PSD from the numerical train passage using WBL88 at 130 km/h and the overall section PSD from the field measurements

4.3 Forces

4.3.1 Measured forces and statistical values

First, it is important to establish the magnitude of the contact forces that are expected at the investigated section. The forces vary from train to train, so the contact forces measured over the past five years (measured approximately twice a year) are therefore used to evaluate the mean and standard deviations of the forces and the force variation over the years, as presented in **Figure 9**. The two most recent measurements were taken after a total update of the catenary system; the system changed from two System 35 sections to one System 20 C1 section. The numerical simulation results from an analysis taking pantograph WBL85 running at 130 km/h, denoted "Abaqus" in **Figure 9**, shows that the obtained values are within the field measurement range. The force varies among the measured train passages, which illustrates the expected random nature of the total process as these measurements are from the same train with the same WBL85 pantograph. This result demonstrates the difficulty of isolating one parameter in practical field testing to set specific values for expected contact forces.

The contact force measurements are from four different positions, and the two lower subfigures in **Figure 9** demonstrate the importance of studying the positions separately. In previous studies, the contact force has been split into rear and front collector force (32,33). In general, the front collector strip clearly experiences a higher contact force than the rear one. The magnitude difference has some variations, which highlights the difficulty of estimating this parameter. The variation between the forces on the front and rear collector strip is clearly not captured by the model, which is natural due to the lack of rotational stiffness perpendicular to the travel direction in the numerical model. A frequency study of the contact forces cannot easily be made because the sampling is spatial

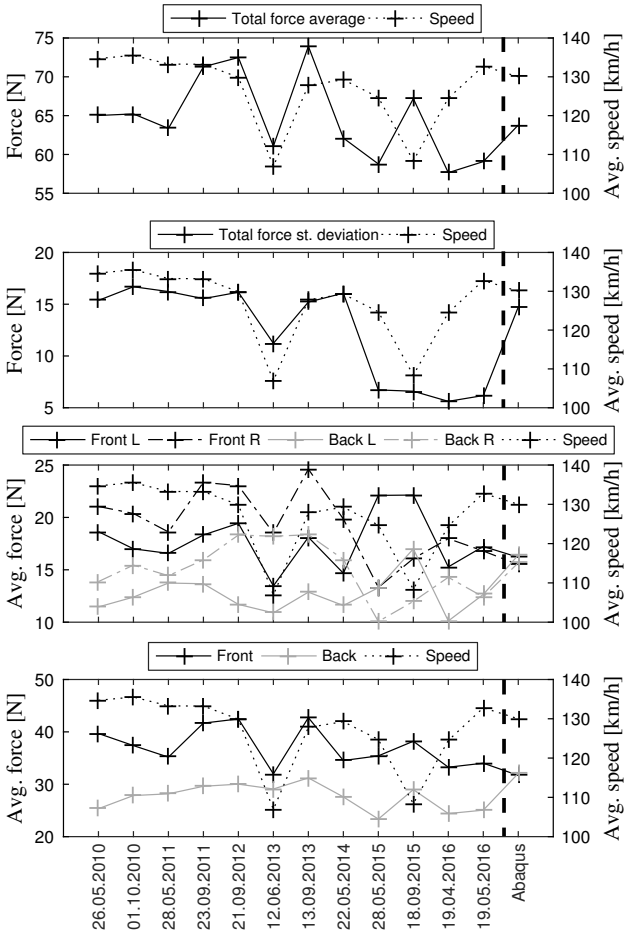

Figure 9. Contact force parameters extracted from twelve measurement runs with Roger 1000 and one numerical simulation

4.3.2 Force variation in output and filtering

The methods used to predict and post-process the contact forces are very important. **Figure 10** shows three different contact force time series, all taken from the same analysis but estimated differently: 1) the force in the actual interface between the contact wire and the collectors strips; 2) the forces from the connectors connecting the pan head to the pan arm; and 3) the previously listed force with the inertia correction described in (14). The differences between these three forces indicate the variation in contact force estimations depending only on how the force is estimated.

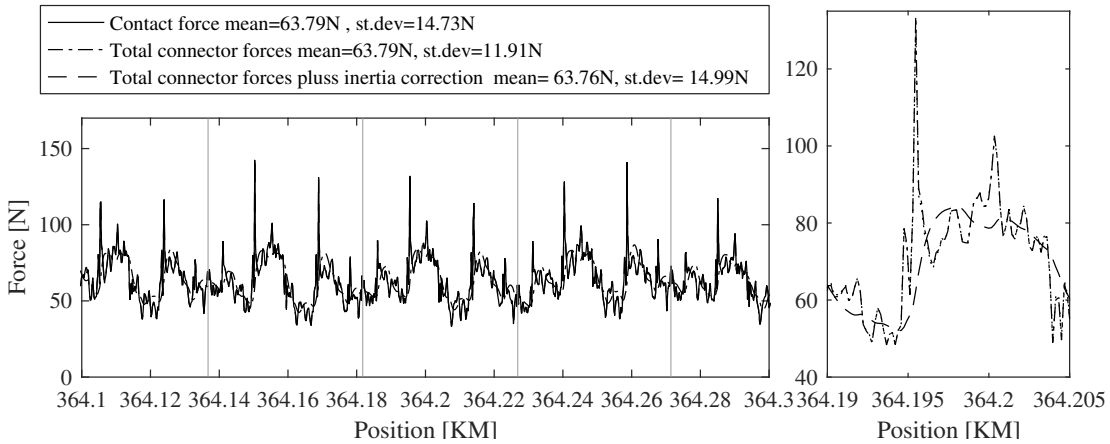

Figure 10. Contact forces from the numerical analysis at 130 km/h with pantograph WBL88. The right part of the figure shows the differences between the connector forces and contact forces on a small part of the section

To further study this effect, the results from the four different numerical simulations, WBL85 and WBL88 pantographs at 80 and 130 km/h, are listed in **Table 4**. This was chosen for presenting a range of different forces. First, "Contact force" is the force measured at the interface between the two collector strips in the model and the contact wire with 200 Hz sampling. Second, "Contact force, filter @ 20 Hz" is calculated as specified in (14), filtering the contact force at 20 Hz. Third, "Connector forces" is the total forces acting in the connectors between the collector strips and the pan arm. Fourth, "Connector forces and accelerations" is the sum of the forces acting in the connectors as well as the inertia correction from (14). Finally, "Connector forces and accelerations, filter @ 20 Hz" is the forces that (14) states should be computed. The filtering was performed using a 5th - order Butterworth low pass filter. It was chosen because it has a magnitude response that is maximally flat in passband and monotonic overall.

In general, the mean values of the contact forces are the same for all of the methods used; the other parameters vary with the prediction method. The unfiltered contact forces and the inertia corrected connector forces give approximately the same results. In general, the inertia corrected forces have a slightly higher standard deviation and maximum values than the contact forces. A significant difference is shown when comparing these two forces to the connector forces. Compared with the unfiltered contact force, the 20 Hz filtered contact force for "Analysis 4" gives a 19% lower standard deviation, a 32% decrease in the maximum value, and a 57% increase in the minimum value. The same trends are clearly shown for all analyses and increase with speed.

Table 4. Tabulated results from the numerical analyses performed on Fokstua wire 21

Analysis	**1**	**2**	**3**	**4**
Pantograph type	WBL85	WBL88	WBL85	WBL88
Speed (km/h)	80	80	130	130
Max. displacement at S1 [mm]	26.38	26.95	34.53	34.57
1. Contact force, mean [N]	58.39	58.39	63.82	63.79
2. Contact force, filter @ 20 Hz, mean [N]	58.39	58.39	63.82	63.79
3. Connector forces, mean [N]	58.37	58.36	63.81	63.79
4. Connector forces + inertia correction, mean [N]	58.37	58.37	63.80	63.76
5. Connector forces + inertia correction, filter @ 20 Hz, mean [N]	58.37	58.37	63.79	63.76
1. Contact force, st. dev. [N]	7.12	7.32	13.93	14.73
2. Contact force, filter @ 20 Hz, st. dev. [N]	6.89	6.97	12.58	13.17
3. Connector forces, st. dev. [N]	6.68	6.45	12.25	11.91
4. Connector forces + inertia correction, st. dev. [N]	7.18	7.41	14.13	14.99
5. Connector forces + inertia correction, filter @ 20 Hz, st. dev. [N]	6.95	7.05	12.77	13.42
1. Contact force, min [N]	34.21	35.19	22.34	21.02
2. Contact force, filter @ 20 Hz, min [N]	34.37	37.46	26.54	25.85
3. Connector forces, min [N]	30.94	35.64	27.82	33.05
4. Connector forces + inertia correction, min [N]	33.53	35.20	22.39	20.89
5. Connector forces + inertia correction, filter @ 20 Hz, min [N]	33.69	36.67	26.57	25.76
1. Contact force, max [N]	85.40	90.00	148.54	154.88
2. Contact force, filter @ 20 Hz, max [N]	82.02	82.85	111.65	105.12
3. Connector forces, max [N]	81.74	81.22	108.77	104.98
4. Connector forces + inertia correction, max [N]	86.24	90.97	150.27	156.56
5. Connector forces + inertia correction, filter @ 20 Hz, max [N]	81.70	83.81	112.04	106.40

A more thorough study on the effect of filtering on the output contact forces is also conducted because of the substantial effects due to filtering on the predicted contact force. The time series from a 130 km/h train passage with a WBL88 pantograph is studied, and the contact force time series is filtered with different low-pass cut-off frequency limits. The selected parameters of this study are the mean, standard deviation, the minimum, and maximum of the contact force. The filtering shows clear effects on the contact force time series. The mean value is approximately unchanged, as expected, but the filtering significantly affects all other parameters. As the filter is set to higher frequencies, the standard deviation and the maximum value increase, while the minimum decreases. The relative change between a 20 Hz cut-off and an 80 Hz cut-off is an 11% increase in standard deviation, a 36% increase in maximum value, and 19% decrease in minimum value. The contact force parameters are presented in **Figure 11**, and the values relative to those found at a 20 Hz cut-off frequency are presented in **Figure 12**.

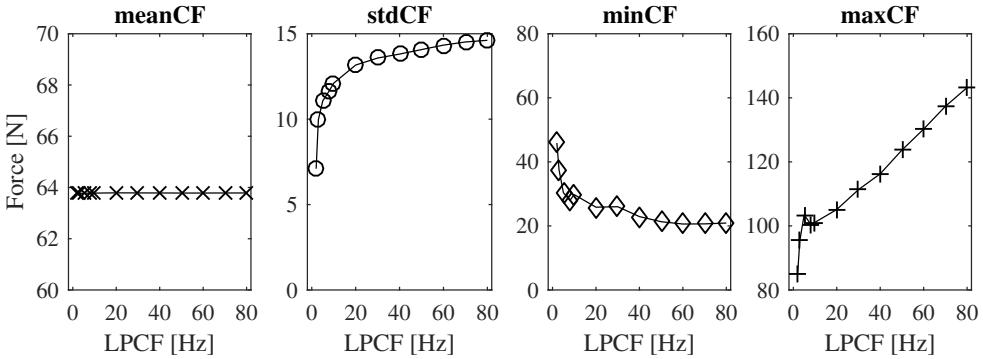

Figure 11. Mean, standard deviation, minimum and maximum of the contact force time series for a 130 km/h train passage with WBL88 pantograph filtered at different low-pass cut-off frequencies (LPCF)

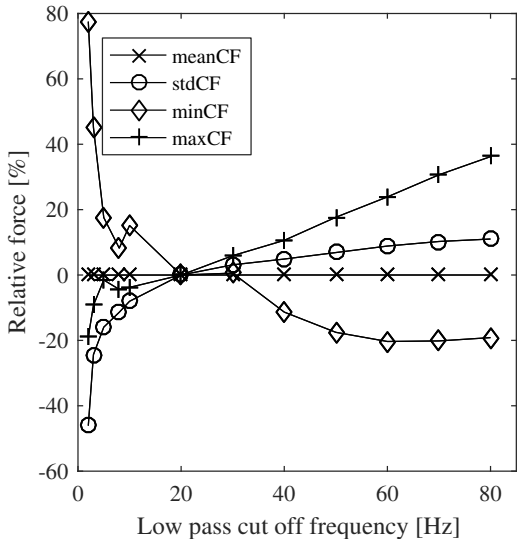

Figure 12. Relative changes in the mean, standard deviation, minimum and maximum of the contact force time series related to the low-pass cut-off frequency limit; the values at 20 Hz are set to 0%

5 Conclusion

This paper investigates the variation in predicting the pantograph-catenary interaction contact force. The investigation analyses both field measurements and numerical simulations. First, the numerical model is validated by comparing the geometry, elasticity, pre-sag, displacement time series, frequency content of the acceleration time series and the statistical contact force values with field measurements. In addition, a description of the numerical model is included. Second, the contact forces from field measurements are studied to demonstrate the variation among individual train passages. In addition, the variation between the front and rear collector strips are shown to be varying and substantial. Third, the variation in the contact force prediction is studied using numerical model results. The standard deviation is stated to be the most important quantity for defining the contact quality (34), which is generally true when regarding the contact quality along a whole section. However, the maximum

and minimum values can help identify point wear, loss of contact, and other local effects that are very important for the local contact quality and for lifetime estimations. The results of this study indicate that the maximum and minimum contact force are more sensitive to filtering than the standard deviation. The mean value is shown to be constant regardless of post-processing for all practical purposes. Comparing the results from an 80 Hz cut-off to the 20 Hz suggested in the standard EN 50317:2012 shows, for one of the analyses, an 11% increase in the standard deviation, a 36% increase in the maximum value and a 19% decrease in the minimum value. These results demonstrate the need for increasing the cut-off frequency limit to study local effects, such as point wear.

Acknowledgements

The authors are grateful to Jernbaneverket, the Norwegian National Rail Administration, for their assistance with field measurements and the funding of this research.

Bibliography

[1] Poetsch G, Evans J, Meisinger R, et al. Pantograph/catenary dynamics and control. Veh Syst Dyn. 1997;28:159–195. doi: 10.1080/00423119708969353.

[2] Kiessling F, Puschmann R, Schmieder A, et al. Contact lines for electric railways : planning, design, implementation, maintenance. 2nd ed. Erlangen: Publicis Publishing. 2012.

[3] Wu TX, Brennan MJ. Dynamic stiffness of a railway overhead wire system and its effect on pantograph–catenary system dynamics. J Sound Vib. 1999;219:483–502. doi: 10.1006/jsvi.1998.1869.

[4] Alberto A, Benet J, Arias E, et al. A high performance tool for the simulation of the dynamic pantograph–catenary interaction. Math Comput. Simul. 2008;79:652–667.

[5] Mei G, Zhang W, Zhao H, et al. A hybrid method to simulate the interaction of pantograph and catenary on overlap span. Veh Syst Dyn. 2006;44:571–580:571–80. doi: 10.1080/00423110600875559.

[6] Lee JH, Park TW, Oh HK, et al. Analysis of dynamic interaction between catenary and pantograph with experimental verification and performance evaluation in new high-speed line. Veh Syst Dyn. 2015;53:1117–1134. doi: 10.1080/00423114.2015.1025797.

[7] Gerstmayr J, Shabana AA. Analysis of thin beams and cables using the absolute nodal Co-ordinate formulation. Nonlin Dyn. 2006;45:109–130. doi: 10.1007/s11071-006-1856-1.

[8] Sanchez-Rebollo C, Jimenez-Octavio JR, Carnicero A. Active control strategy on a catenary–pantograph validated model. Veh Syst Dyn. 2013;51:554–569. doi: 10.1080/00423114.2013.764455.

[9] Pappalardo CM, Patel MD, Tinsley B, et al. Contact force control in multibody pantograph/catenary systems. Proc Inst Mech Eng E J Multi-Body Dyn. 2015:1–22. doi: 10.1177/1464419315604756.

[10] Ikeda M, Nagasaka S, Usuda T. A precise contact force measuring method for overhead catenary system. Proceedings of World Congress on Railway Research. Köln: UIC; 2001; Available from: http://www.railway-research.org/IMG/pdf/015.pdf.

[11] Usuda T. The pantograph contact Force measurement method in overhead catenary system. Proceedings of the 8th World Congress on Railway Research. Seoul. South Korea: UIC; 2008. Available from: http://www.railway-research.org/IMG/pdf/s.1.4.3.4.pdf.

[12] Zhang W, Shen Z, Zeng J. Study on dynamics of coupled systems in high-speed trains. Veh Syst Dyn. 2013;51(7):966–1016. doi: 10.1080/00423114.2013.798421.

[13] Bucca G, Collina A. Electromechanical interaction between carbon-based pantograph strip and copper contact wire: A heuristic wear model. Tribol Int. 2015;92:47–56. doi: 10.1016/j.triboint.2015.05.019.

[14] NEK. NEK EN 50317:2012 Railway applications - Current collection systems - Requirements for and validation of measurements of the dynamic interaction between pantograph and overhead contact line. 2012.

[15] Ambrósio J, Pombo J, Rauter F, et al. A memory based communication in the co-simulation of multibody and finite element codes for pantograph-catenary interaction simulation multibody dynamics. In: Bottasso CL, editor. Multibody dynamics computational methods and applications. Netherlands: Springer Verlag; 2009. p. 231–252.

[16] Collina A, Bruni S. Numerical simulation of pantograph-overhead equipment interaction. Veh Syst Dyn. 2002;38:261–291. doi: 10.1076/vesd.38.4.261.8286.

[17] Nåvik P, Rønnquist A, Stichel S. The use of dynamic response to evaluate and improve the optimization of existing soft railway catenary systems for higher speeds. Proc Inst Mech Eng Part F J Rail Rapid Transit. 2015;230:1388–96.

[18] Rønnquist A, Nåvik P. Dynamic assessment of existing soft catenary systems using modal analysis to explore higher train velocities: a case study of a Norwegian contact line system. Veh Syst Dyn. 2015;53:756–774. doi: 10.1080/00423114.2015.1013040.

[19] Bruni S, Ambrosio J, Carnicero A, et al. The results of the pantograph–catenary interaction benchmark. Veh Syst Dyn. 2015;53:412–435. doi: 10.1080/00423114.2014.953183.

[20] Nåvik P, Rønnquist A, Stichel S. A wireless railway catenary structural monitoring system: full-scale case study. Case stud. Struct Eng. 2016;6:22–30.

[21] Frøseth GT, Nåvik P, Rønnquist A. Close Range Photogrammetry for Measuring the Response of a Railway Catenary System. Proceedings of the Third International Conference on Railway Technology: Research, Development and Maintenance, ed. J. Pombo. Civil-Comp Press, Stirlingshire, UK, Paper 102. 2016. doi: 10.4203/ccp.110.102.

[22] Rønnquist A, Nåvik P. Exploring Dynamic Behaviour of Soft Catenaries subject to Regular Loading using Full Scale Measurements. Proceedings of the Third International Conference on Railway Technology: Research, Development and Maintenance, ed. J. Pombo. Civil-Comp Press, Stirlingshire, UK, Paper 101. 2016. doi: 10.4203/ccp.110.101.

[23] Nåvik P, Rønnquist A, Stichel S. Identification of system damping in railway catenary wire systems from full-scale measurements. Eng Struct. 2016;113:71–78. doi: 10.1016/j.engstruct.2016.01.031.

[24] Mekanisk systembeskrivelse av kontaktledningsanlegg [Internet]. The Norwegian National Rail Administration; [cited 2013 Oct 2]. Available from: http://www.jernbanekompetanse.no/wiki/Mekanisk_systembeskrivelse_av_kontaktledningsanlegg.

[25] NEK. NEK EN 50318:2002 Railway applications - Current collection systems - Validation of simulation of the dynamic interaction between pantograph and overhead contact line. 2002.

[26] Carnevale M, Facchinetti A, Maggiori L, et al. Computational fluid dynamics as a means of assessing the influence of aerodynamic forces on the mean contact force acting on a pantograph. Proc Inst Mech Eng Part F J Rail Rapid Transit. 2016;230:1698-1713. doi: 10.1177/0954409715606748.

[27] Song Y, Liu Z, Wang H, et al. Nonlinear analysis of wind-induced vibration of high-speed railway catenary and its influence on pantograph–catenary interaction. Veh Syst Dyn. 2016;54:723–747. doi: 10.1080/00423114.2016.1156134.

[28] ABAQUS 6.14 Theory Manual. Dassault Systèmes; 2014

[29] Ambrósio J, Pombo J, Pereira M, et al. Recent developments in pantograph-catenary interaction modelling and analysis. Int J Railw Technol. 2012;1:249–278. doi: 10.4203/ijrt.1.1.12.

[30] ROGER 1000 [Internet]. [cited 2016 Jun 16]. Available from: http://www.mermecgroup.com/inspect/recording-cars/104/roger-1000.php.

[31] BANVERKET. Analys av kontaktledningsdynamik vid flera verksamma strömavtagare Del 1, BKL 02/10. Banverket 2004.

[32] Carnevale M, Collina A. Processing of collector acceleration data for condition-based monitoring of overhead lines. Proc Inst Mech Eng Part F J Rail Rapid Transit. 2016;230:472–85. doi: 10.1177/0954409714545637

[33] Zhou N, Zhang W, Li R. Dynamic performance of a pantograph-catenary system with the consideration of the appearance characteristics of contact surfaces. J Zhejiang Univ Sci A. 2011;12:913–920. doi: 10.1631/jzus.A11GT015.

[34] Ambrósio J, Pombo J, Pereira M. Optimization of high-speed railway pantographs for improving pantograph-catenary contact. Theor Appl Mech Lett. 2013;3:013006. doi:10.1063/2.1301306.